

# Mining Latent Relationships among Clients: Peer-to-peer Federated Learning with Adaptive Neighbor Matching

Zexi Li, Jiaxun Lu, *Member, IEEE*, Shuang Luo, Didi Zhu, Yunfeng Shao, *Member, IEEE*,  
Yinchuan Li, *Member, IEEE*, Zhimeng Zhang, and Chao Wu

**Abstract**—In federated learning (FL), clients may have diverse objectives, merging all clients' knowledge into one global model will cause negative transfers to local performance. Thus, clustered FL is proposed to group similar clients into clusters and maintain several global models. Nevertheless, current clustered FL algorithms require the assumption of the number of clusters, they are not effective enough to explore the latent relationships among clients. However, we take advantage of peer-to-peer (P2P) FL, where clients communicate with neighbors without a central server and propose an algorithm that enables clients to form an effective communication topology in a decentralized manner without assuming the number of clusters. Additionally, the P2P setting will release the concerns caused by the central server in centralized FL, such as reliability and communication bandwidth problems. In our method, 1) we present two novel metrics for measuring client similarity, applicable under P2P protocols; 2) we devise a two-stage algorithm, in the first stage, an efficient method to enable clients to match same-cluster neighbors with high confidence is proposed; 3) then in the second stage, a heuristic method based on Expectation Maximization under the Gaussian Mixture Model assumption of similarities is used for clients to discover more neighbors with similar objectives. We make a theoretical analysis of how our work is superior to the P2P FL counterpart and extensive experiments show that our method outperforms all P2P FL baselines and has comparable or even superior performance to centralized cluster FL. Moreover, results show that our method is much effective in mining latent cluster relationships under various heterogeneity without assuming the number of clusters and it is effective even under low communication budgets.

**Index Terms**—Federated learning, peer-to-peer communication, distributed learning, clustering.

## 1 INTRODUCTION

Federated learning (FL) [1], [2], [3], [4], [5] facilitates collaborative training among a set of clients while preserving privacy so that clients can reach a better performance than individual training. Heterogeneity is an inherent problem in federated learning, since clients may have diverse optimization objectives (learning tasks) [6].

There may exist a cluster structure among clients, a small group of clients have similar data distributions, thus their optimization objectives are consistent, while there is dominant inconsistency among different groups. It is very common in applications such as recommendation systems [7], [8]. Therefore, clustered FL methods [9], [10], [11], [12] are proposed for better personalization by grouping clients into clusters and maintaining a global model in each cluster. The main challenge of clustered heterogeneity is that the latent similarity relationships among clients are unknown. Existing clustered FL researches adopt the conventional server-client communication pattern and estimate clients'

cluster identities by iterative [9] or hierarchical [11] methods. However, there are mainly three concerns: (1) Current clustered FL algorithms require the assumption of the number of clusters, it is not effective enough to explore the latent relationships among clients. If the assumed number of clusters is set inappropriately, outliers in a cluster will hinder overall performance. (2) The central server in the current setup bears a potential risk of weakness, the distributed system will break down if it is under malicious attack. (3) If the number of clients is enormous, the central server requires large communication bandwidth [13]. Although the pressure of bandwidth can be relieved by reducing the number of participated clients in each round, it may result in poor convergence in cluster identity estimations.

Consequently, we take advantage of peer-to-peer (P2P) FL where clients communicate with neighbors without a central server and propose a P2P FL algorithm: Personalized Adaptive Neighbour Matching (PANM), providing a robust and effective method to personalized clustered FL in a decentralized manner. We solve the node clustering problem into a binary classification problem: from the perspective of the client-side, each client only needs to estimate an accessible client is whether in the same cluster as itself or not. Once the neighbor estimation is correct, a clustered communication topology will be inherently established without assuming the number of clusters. Hence, PANM is effective enough to explore the latent relationships among clients.

We note that in previous works, most P2P FL algorithms assume random or fixed communication topologies [14],

- Zexi Li and Didi Zhu are with the College of Computer Science and Technology, Zhejiang University, Hangzhou, China. E-mail: {zexi.li, didi\_zhu}@zju.edu.cn.
- Jiaxun Lu, Yunfeng Shao and Yinchuan Li are with Huawei Noah's Ark Lab, Beijing, China. E-mail: {lujiaxun, shaoyunfeng, liyinchuan}@huawei.com.
- Chao Wu and Shuang Luo are with the School of Public Affairs, Zhejiang University, Hangzhou, China. E-mail: {luoshuang, chao.wu}@zju.edu.cn.
- Zhimeng Zhang is with the School of Software Technology, Zhejiang University, Hangzhou, China. E-mail: zhimeng@zju.edu.cn.
- Corresponding Author: Chao Wu.

[15] and they focus on reaching the global consensus by optimization techniques [16], [17]. We will show in the experiments that the random and fixed communications will hamper personalization when the objectives of clients are divergent which is realistic in FL scenarios. In addition, there is no global consensus in clustered heterogeneity, but there may exist partial consensus in each cluster. Therefore, our method PANM realizes the construction of adaptive communication topologies in P2P FL, by which clients will achieve partial consensus in the group that shares similar objectives. To the best of our knowledge, this is the first P2P FL algorithm that takes divergent objectives among clients into consideration.

Overall, there are two stages in PANM. In stage one, PANM enables clients to initialize neighbors with high confidence of being same-cluster. In stage two, a heuristic method based on Expectation Maximization (EM) is adopted to enable clients to identify the rest of same-cluster peers and take them as neighbors. The heuristic EM-based method is formulated under the Gaussian Mixture Model assumption of similarities. Our main contributions are as follows.

- We propose two efficient, effective, and privacy-preserving metrics to evaluate the pair-wise similarity of client objectives in P2P FL. They are based on losses and gradients, respectively.
- We present a novel P2P FL algorithm: PANM, which enables clients to match neighbors with consistent objectives (same cluster identity), improving local performance.
- We devise two stages in PANM: confident neighbor initialization and heuristic neighbor matching based on EM. We provide a theoretical analysis of how our method is superior to the P2P FL counterpart.
- We conduct extensive experiments on a spectrum of Non-IID degrees and network settings, using different datasets. It is shown that PANM outperforms all P2P baselines including Oracle (with prior knowledge of cluster identities). Compared with centralized clustered FL algorithms, PANM is more effective in exploring latent cluster structure and has comparable, even better performance.
- Additionally, even under low communication budgets, PANM can still achieve superior performance to baselines.

The rest of this paper is organized as follows. Section 2 presents related works in clustered FL and P2P FL. Section 3 shows the motivation and the design of PANM, including two metrics for measuring client similarity in P2P FL, the first-stage confident neighbor initialization, and the second-stage heuristic neighbor matching. We also incorporate some theoretical analyses in Section 3. Results of extensive experiments are shown and analyzed in Section 4. We provide further discussion in Section 5. Then we conclude the paper in Section 6.

## 2 RELATED WORKS

**Clustered Federated Learning.** Clustered FL holds the Non-IID assumption that different groups of clients have

their own optimization objectives of learning tasks, aggregating models in the same cluster will bring better personalization while aggregating models in inconsistent clusters will cause negative transfers. Current clustered FL researches are mainly under a centralized manner.

Hierarchical clustering methods are used to achieve better personalization. Sattler *et al.* [11] use a hierarchical optimal bi-partitioning algorithm based on cosine similarity of weights or gradients. However, the bi-partitioning method bears high computation costs and requires multiple communication rounds to completely separate all clients with different objectives. Further, Briggs *et al.* [18] design a hierarchical algorithm for a wider range of Non-IID settings and it reduces clustering to a single step to lower computation and communication loads. But it also requires iteratively calculating pair-wise distances between different clusters, which is computationally complex.

In addition, methods derived from K-means are used to recognize clients' cluster identities. FedSEM [10] uses K-means to cluster clients based on clients'  $l_2$  distances of model weights. Nonetheless,  $l_2$  distance often suffers from high-dimension, low-sample-size situation which is known as distance concentration phenomenon in high dimension [19]. To solve the efficiency problem of cluster estimation, Ghosh *et al.* [9] propose an iterative algorithm IFCA which incorporates the essence of K-means, IFCA keeps several global models and clients iteratively choose which global model it is prone to contribute to based on local losses of global models. IFCA requires high communication costs, for it needs to broadcast all global models in each round and it is sensitive to the initialization. We also notice that for IFCA, partial participation of clients in each round may result in poor convergence. Besides, Duan *et al.* [12], [20] use decomposed cosine similarity of models' updates to group clients and makes both intra-cluster and inter-cluster aggregations and design an efficient newcomer device cold start mechanism. K-means clustering is inherently used in their works.

Note that, all the above-mentioned algorithms in clustered FL are not effective enough in exploring latent relationships among clients. They highly rely on the level of hierarchy or the assumption of the number of clusters, however, these are latent and cannot be obtained as prior knowledge.

**Peer-to-peer Federated Learning.** Peer-to-peer federated learning (P2P FL, also known as decentralized FL) alters the centralized topology of conventional FL, it allows clients to communicate with limited neighbors [14], [21]. There is a study comparing decentralized algorithms like gossip learning with centralized federated learning in terms of communication efficiency, it is found that the best gossip variants perform comparably to the best centralized federated learning overall [22]. Early works related to P2P FL introduce the P2P FL problem under privacy constraints and provide theoretical guarantees; Lalitha *et al.* [14], [15] use a Bayesian-like approach to let clients collectively learn a model that best fits the observations over the entire network; and Bellet *et al.* [23] make P2P FL differentially private and analyze the trade-off between utility and privacy. They mainly study P2P FL under IID data assumption, but heterogeneity is prevalent in FL practices.

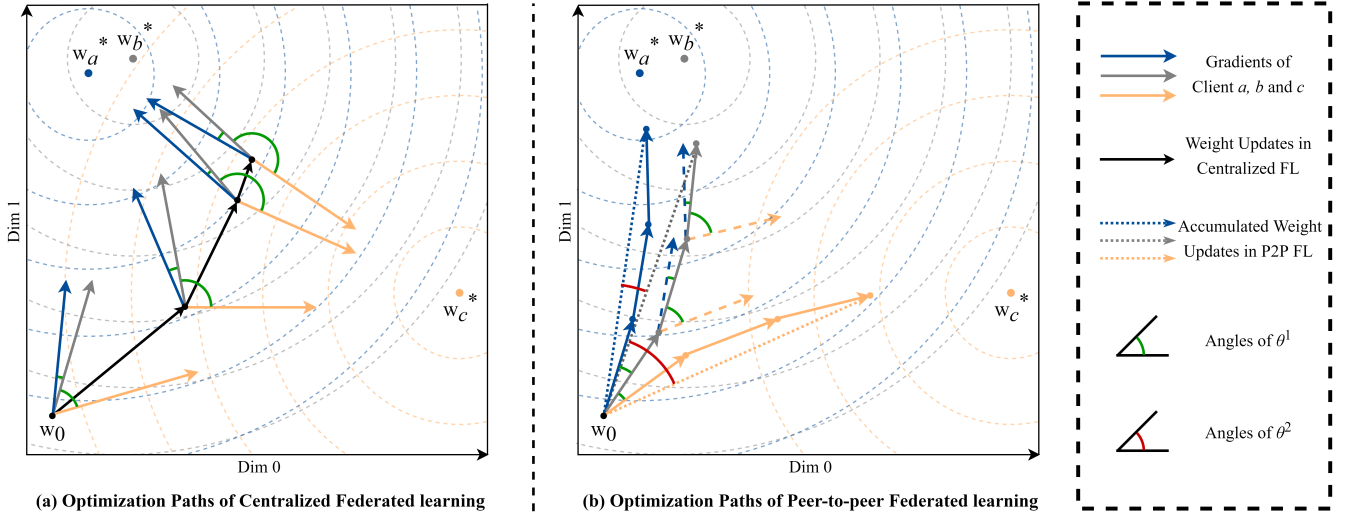


Fig. 1: Schematic diagram of optimization paths in centralized FL (a) and P2P FL (b), respectively. In the figure, objective of client  $a$  is similar with client  $b$  and dissimilar with client  $c$ .

Recent works mostly discuss class imbalance heterogeneity and communication problems. First, to tackle class imbalance, Li *et al.* [24] use mutual knowledge distillation instead of weight averaging, Bellet *et al.* [25] elaborately design a topology from holistic perspective. However, without a central server, the holistic perspective is impractical, it is hard for clients to form such a topology with limited observations. Second, communication of P2P FL can be more efficient by sparsification [26], adaptive partial gradient aggregation [27], and using max-plus linear system theory to compute throughput [28].

Most recently, swarm learning [21] is brought up as a P2P FL customized for medical researches, utilizing edge computing and blockchain as infrastructures, and it attracts wide attention. It provides strong application practices of P2P FL. While we are formulating this paper, we find a related same-time work (PENS) that has the same motivation as ours but uses different methods [29]. PENS adopts a two-stage strategy. In stage one, in each round, clients choose top  $k$  peers as neighbors for aggregation from randomly sampled  $l$  neighbor candidates. After stage one, clients select the peers that were chosen as neighbors more than “the expected amount of times” in stage one as *permanent neighbors*. In stage two, in each round, clients randomly choose  $k$  neighbors for aggregation from *permanent neighbors*. It is very possible for PENS to have noisy neighbor estimations, we analyze the superiority of PANM to PENS in Section 3 and 4.

### 3 METHOD

#### 3.1 Notation and Setting

We formulate it as an empirical risk minimization problem, and the distributed optimization objective is in the sum-structured form  $f : \mathbb{R}^d \rightarrow \mathbb{R}$ , as

$$f^* := \min_{\mathbf{w}_1, \dots, \mathbf{w}_i \in \mathbb{R}^d} \left[ \frac{1}{n} \sum_{i=1}^n f_i(\mathbf{w}_i) \right], \quad (1)$$

where there are  $n$  clients in the system. The  $f_i : \mathbb{R}^d \rightarrow \mathbb{R}$  is the loss function of client  $i$  ( $i \in \{1, \dots, n\}$ ) on its local dataset, given by:  $f_i(\mathbf{w}) := \mathbb{E}_{\xi \sim \mathcal{D}_i} [F_i(\mathbf{w}, \xi)]$ , where  $\mathcal{D}_i$  denotes the local data distribution of client  $i$ . In P2P FL setting, each client  $i$  maintains its local parameter weights  $\mathbf{w}_i^t \in \mathbb{R}^d$ , and updates them as

$$\mathbf{w}_i^{t+1} = \sum_{j \in \mathcal{N}_i^{t'}} w_{i,j} (\mathbf{w}_j^t - \eta \nabla F_j(\mathbf{w}_j^t, \xi_j)) + w_{i,i} (\mathbf{w}_i^t - \eta \nabla F_i(\mathbf{w}_i^t, \xi_i)), \quad (2)$$

where  $\xi_j \sim \mathcal{D}_j$ .  $\mathcal{N}_i^{t'}$  is the round  $t$ 's aggregation neighbors of client  $i$ , randomly sampled from the neighbor list  $\mathcal{N}_i^t$ ,  $\mathcal{N}_i^{t'} \in \mathcal{N}_i^t$ . The size of  $\mathcal{N}_i^{t'}$  is  $k$ , while the size of  $\mathcal{N}_i^t$  is  $m$ ,  $k \leq m$ .  $w_{i,j}$  denotes the importance weight of client  $j$  to client  $i$ . In this paper, we set  $w_{i,j} = w_{i,i} = \frac{1}{k+1}$ . Equation (2) shows the process of one communication round in P2P FL.

#### 3.2 Algorithm

##### 3.2.1 Metrics for Measuring Client Similarity

Metrics for measuring the consistency of optimization objectives are needed to enable clients to select same-cluster peers and filter out outliers. However, due to privacy concerns, in FL, we cannot use data distance measurements like maximum mean discrepancy distance [30], since sharing data is forbidden. Loss evaluation is a simple metric, commonly used in the literature [9], [29]. By evaluating other clients' models on local data, the model with lower loss value is more possible to have a similar learning task. For P2P FL, we can formulate the similarities based on loss as

$$s_{i,j} = 1/F_i(\mathbf{w}_j^t, \xi_i), \quad (3)$$

where  $s_{i,j}$  is similarity between client  $i$  and  $j$ ,  $\xi_i \sim \mathcal{D}_i$ . Since this metric is simple, we adopt this metric in our PANM (named as PANMLoss).

However, calculating loss value is computation-consuming because it requires inferring models on the

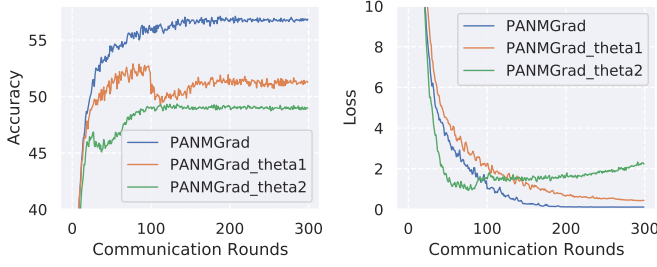


Fig. 2: Ablation study of PANMGrad. CIFAR10 with two rotations  $\{0^\circ, 180^\circ\}$ , 50 clients in each cluster,  $l = 10, k = 5$ , trainset size is 400. PANMGrad refers to PANM with metric based on cosines of  $\theta_1$  and  $\theta_2$ , PANMGrad-theta1 refers to PANM with metric based on  $\theta_1$ , PANMGrad-theta2 refers to PANM with metric based on  $\theta_2$ .

training dataset. Moreover, local data may not be available for extra computation. Hence, we develop a more efficient metric based on gradients and accumulated weight updates.

In centralized clustered FL, Sattler *et al.* [11] use the cosine similarity of gradients to measure the consistency of optimization objectives, the function can be formulated as

$$\cos \theta_{i,j}^1 = \frac{\langle \mathbf{w}_i^t - \mathbf{w}_i^{t-1}, \mathbf{w}_j^t - \mathbf{w}_j^{t-1} \rangle}{\|\mathbf{w}_i^t - \mathbf{w}_i^{t-1}\| \cdot \|\mathbf{w}_j^t - \mathbf{w}_j^{t-1}\|}, \quad (4)$$

where  $\theta^1$  refers to the angle of vectorized gradients,  $\mathbf{w}_i^t - \mathbf{w}_i^{t-1}$  refers to the gradients in the local updates of round  $t$ . In centralized FL, models are initialized as the same global model at the beginning of local training in each round ( $\mathbf{w}_i^{t-1} = \mathbf{w}_j^{t-1} = \mathbf{w}^{t-1}$ ), so the cosine function of gradients can effectively imply the consistency, as shown in (a) of Figure 1. Although in P2P FL, without the central server, client model weights diverge since the first round, the measurement of gradients will be noisy, the angle of gradients is shown as  $\theta^1$  in (b) of Figure 1.

To solve this issue, we notice the accumulated weight updates from the initial model can signify the history optimization directions, and the cosine similarity of the weight updates can imply the consistency of objectives to some extent

$$\cos \theta_{i,j}^2 = \frac{\langle \mathbf{w}_i^t - \mathbf{w}_0, \mathbf{w}_j^t - \mathbf{w}_0 \rangle}{\|\mathbf{w}_i^t - \mathbf{w}_0\| \cdot \|\mathbf{w}_j^t - \mathbf{w}_0\|}. \quad (5)$$

The angle of accumulated weight updates is  $\theta^2$  in (b) of Figure 1.

According to Equation (4) and (5), we combine the cosine similarities of  $\theta^1$  and  $\theta^2$  to formulate our new metric as

$$s_{i,j} = \alpha \cos \theta_{i,j}^1 + (1 - \alpha) \cos \theta_{i,j}^2, \quad (6)$$

where  $\alpha$  is the hyperparameter controlling the weight of two cosine functions, we set  $\alpha = 0.5$  in our experiments. Notably, our new metric is robust and effective in the P2P FL setting.

Experiments in Figure 2 show that the metric combining two cosine functions in Equation 6 can significantly enhance the effectiveness of similarity measurements, compared with using one function alone. We explain that: if using  $\cos \theta^1$  alone, it will be very noisy since the models

are not synchronized. If using  $\cos \theta^2$  alone, clients which are communicated with in the previous rounds will have similar weights, so they are more prone to have high similarities, but if previous neighbors include outliers, they are also likely to be next-round neighbors. However, these two functions are complementary, the combination can improve performance. For the clients with high  $\cos \theta^1$  similarity,  $\cos \theta^2$  will imply the history of accumulated weight updates, if the  $\cos \theta^2$  similarity is high, the clients are more likely to be same-cluster. For the clients with high  $\cos \theta^2$  similarity, they have similar weights, and  $\cos \theta^1$  is more effective when weights are similar (this case is similar to the centralized FL cases, where common model initialization in each round can make  $\cos \theta^1$  more effective). Thus, the combination of the two functions can more robustly imply the similarities. We adopt the metric in Equation (6) in PANM, notated as PANMGrad.

Additionally, the similarity computed by Equation (3) is nearly symmetric: if two clients have distinct objectives, then cross-validation losses on both sides are high, but they are not necessarily equal; while the metric in Equation (6) is completely symmetric because the inner product operation is symmetric. Symmetric metrics are beneficial to enable clients to reach consensus, which means that our newly proposed metric is superior.

### 3.2.2 Confident Neighbor Initialization

Based on the similarity metrics mentioned in the last subsection, we can devise our P2P FL algorithm PANM. We introduce the first stage of PANM in this subsection.

In the first stage of P2P FL training, clients have to initialize their collaborative neighbors from random sampled peers ( $C_i^t, |C_i^t| = l$ ). In PENS [29], clients select top  $k$  peers with maximum similarity as neighbors in each round

$$\begin{aligned} N_i^t &= \arg \max_N \sum_{j \in N} s_{i,j} \\ s.t. \quad N &\not\subseteq C_i^t, |N| = k. \end{aligned} \quad (7)$$

Nevertheless, the probability that all the initialized neighbors are same-cluster is relatively low. Hence, we propose a more confident method: the Confident Neighbor Initialization (CNI) algorithm. In CNI, after the first round, we add the neighbors in the previous round to the candidate list in the current round (as shown in Equation 8), consequently, the confidence of same-cluster neighbors increases over round.

$$\begin{aligned} N_i^t &= \arg \max_N \sum_{j \in N} s_{i,j} \\ s.t. \quad N &\not\subseteq C_i^t \cup N_i^{t-1}, t > 1, |N| = k. \end{aligned} \quad (8)$$

To show the effectiveness of CNI, we provide theoretical analysis, while making the following assumption.

**Assumption 1.** The metrics in Equation (6) and (3) are effective enough, so that for client  $i$  ( $\forall i \in \{1, \dots, n\}$ ), we have:

$$s_{i,p} > s_{i,q} \quad \forall p \in SC_i, q \in DC_i. \quad (9)$$

where  $SC_i$  refers to all the clients that are in the same cluster as client  $i$ , and  $DC_i$  refers to all the clients that are in different clusters with client  $i$ .

Given Assumption 1, we can provide the probability that all the  $k$  neighbors are same-cluster in the round  $t$  when conducting CNI. We assume there are  $n$  clients in the system (including client  $i$ ) and  $a$  clients in the same cluster as client  $i$  (including client  $i$ ), so we can infer the following theorem.

**Theorem 1.** Under Assumption (1), in the round  $t$  when conducting CNI as Equation (8), for client  $i$ , the probability that all the  $k$  neighbors are same-cluster are  $P^t(k)$ , we have

$$\begin{aligned} P^t(k) &= G(k) * P^{t-1}(k) + R(k) \\ &\dots \\ P^2(k) &= G(k) * P^1(k) + R(k) \\ P^1(k) &= R(k). \end{aligned} \quad (10)$$

where  $R(x)$  and  $G(x)$  are two functions and the  $'*$ ' refers to the discrete convolution computation, defined as

$$\begin{aligned} R(x) &= \frac{l!(n-l-1)!}{(n-1)!} \sum_{s=0}^{l-x} \frac{(a-1)!(n-a)!}{s!(l-s)!(n-a-s)!(a-l+s-1)!} \\ G(x) &= \frac{l!(a-1)!(n-a)!(n-l-1)!}{x!(n-1)!(l-x)!(a-x-1)!(n-a-l+x)!} \\ G(x) * P(x) &= \sum_{m=0}^{x-1} G(m)P(x-m). \end{aligned}$$

If conducting PENS as Equation (7), the probability is

$$P^t(k) \equiv R(k). \quad (11)$$

Based on Theorem 1, we provide the following corollary.

**Corollary 1.** Given Theorem 1, we define a function:

$Q(t) = P^t(k), t \in \{1, \dots, T\}$ . The function  $Q(t)$  of CNI is monotone increasing, so we have

$$Q(t) > Q(t-1) > \dots > Q(2) > Q(1). \quad (12)$$

The function  $Q(t)$  of PENS satisfies

$$Q(t) = Q(t-1) = \dots = Q(1) = R(k). \quad (13)$$

**Note 1.** We note that Assumption 1 is strong, and we provide this assumption just for theoretical analysis in Theorem 1 and Corollary 1. We will show in Figure 3 that in practice when Assumption 1 is not strictly held, results are still consistent and similar to the theoretical findings.

The Corollary 1 shows that: by CNI, the probability increases over round, while PENS keeps it unchanged at a low value. Intuitively, we calculate the theoretical probabilities and compare them with experimental results in Figure 3. It is obvious to see that CNI enables PANM to have highly confident neighbors only after several rounds, while the precision of same-cluster neighbors in PENS stays low. However, there are gaps between theory and practice, we explain: at the beginning of distributed training, the models are randomly initialized (not well-trained), therefore the similarity measurements are so noisy that Assumption 1 may not be held. After some rounds, when the similarity metrics are effective enough, the results will be closer to the theoretical findings.

Besides the high confidence of neighbors being same-cluster, CNI also facilitates clients to match the clients with global maximum similarities. Experiments in Section 4 will show it can boost personalization even better than Oracle.

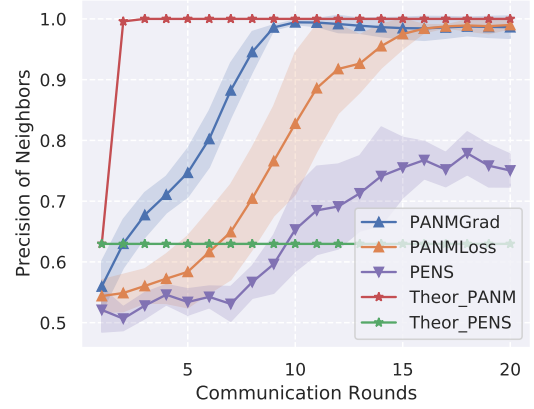


Fig. 3: Precision of same-cluster neighbors in stage 1. CI-FAR10,  $n = 100, l = 10, k = 5$ , two clusters are formed by rotations  $\{0^\circ, 180^\circ\}$ .

### 3.2.3 Heuristic Neighbor Matching

After confident neighbor initialization, we enable clients to have few neighbors with high precision of being same-cluster. For clustered FL, the recall of clustering is also important, since each client needs to find out the whole community with the same objective. Thus, in the second stage of PANM, we use heuristic neighbor matching to facilitate clients to discover more peers with consistent objectives.

In the second stage of PENS, clients choose peers that are selected more than “the expected amount of times” in stage one as neighbors. Theorem 1 implies that if the setting is difficult, stage-one neighbors of PENS are prone to be noisy, afterward in stage two, the matched neighbors are more likely to include outliers. Besides, PENS requires the hyperparameter “the expected amount of times”; without prior knowledge of cluster information, it is hard to set the hyperparameter to an appropriate value. Therefore, in stage two of PANM, we propose a more effective method based on expectation maximization (EM).

It is obvious that for a client, the same-cluster clients may have high similarities while the ones of the different-cluster are low, so we assume the similarities of the same-cluster obey a consistent distribution while the similarities of the different-cluster obey another distribution. The assumption is as follows.

**Assumption 2.** For client  $i$  ( $\forall i \in \{1, \dots, n\}$ ), the similarities between same-cluster clients and client  $i$  obey a Gaussian distribution, parameterized by  $\mathcal{N}(\mu_0, \sigma_0^2)$ , and the similarities between different-cluster clients and client  $i$  obey another Gaussian  $\mathcal{N}(\mu_1, \sigma_1^2)$ , as

$$\begin{aligned} s_{i,p} &\sim \mathcal{N}(\mu_0, \sigma_0^2), s_{i,q} \sim \mathcal{N}(\mu_1, \sigma_1^2) \\ &\forall p \in SC_i, q \in DC_i. \end{aligned}$$

We have  $\mu_0 > \mu_1$ .

Assumption 2 is quite natural in clustered FL, as in Figure 4, the distributions of similarities after stage one of PANM are shown; intuitively, the distributions satisfy our assumption, for there are two distinct Gaussians.



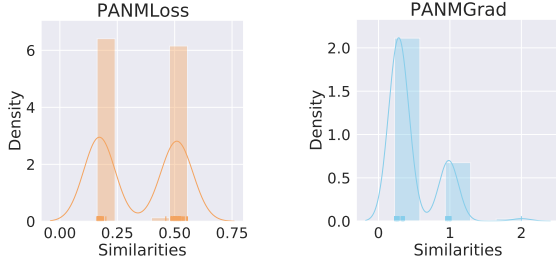


Fig. 4: Distributions of similarities. Similarities between client 1 and other clients are shown. CIFAR10,  $n = 100$ , clusters are formed by rotations  $\{0^\circ, 180^\circ\}$ .

By far, we can formulate the neighbor matching problem into a Gaussian Mixture Model (GMM) problem, a typical solution to GMM problem is EM algorithm. But conventional EM algorithm is not suitable to solve this problem, under the following considerations: (1) Conventional EM method requires calculating probabilities of all data points in one EM step, but for P2P FL, clients only can communicate with several neighbors in one round; (2) The focus of conventional EM solving GMM problem is to accurately estimate the parameters of Gaussians while our focus is to accurately discriminate cluster identities. Additionally, EM algorithms are sensitive to initialization, better initialization makes it more possible to converge to the global optimum.

To tackle above mentioned matters, we devise our Heuristic Neighbor Matching (HNM) algorithm. In each round, client  $i$  randomly samples neighbor candidate list  $C_i^t$  ( $|C_i^t| = l$ ) from non-neighbor clients and also samples a selected neighbor list  $S_i^t$  ( $|S_i^t| = l$  if  $|N_i^t| > l$ , else  $S_i^t = N_i^t$ ) from neighbor clients  $N_i^t$ ; client  $i$  communicate with these clients and compute similarities  $y_j = s_{i,j}$ ,  $j \in M_i^t = C_i^t \cup S_i^t$ . According to Assumption 2, there are two Gaussian distributions in these similarities, the one with higher mean center refers to the same-cluster clients ( $\mathcal{N}(\mu_0, \sigma_0^2)$ ), another one refers to the different-cluster ( $\mathcal{N}(\mu_1, \sigma_1^2)$ ). Assuming the observed data  $y_j$ ,  $j \in M_i^t$  are generated by the Gaussian Mixture Model:

$$\Pr(y|\Theta) = \sum_{r=0}^1 \beta_r \phi(y|\Theta_r). \quad (14)$$

Here,  $\beta_r$  refers to the probability that  $y$  is generated by distribution  $r$ , and  $\Theta = (\beta_0, \beta_1; \Theta_0, \Theta_1)$ . Our target is using EM algorithm to estimate the distribution identities of  $y_j$ , given by

$$\gamma_{j,r} = \begin{cases} 1, & \text{if } j \text{ belongs to distribution } \mathcal{N}_r \\ 0, & \text{otherwise.} \end{cases}$$

where  $j \in M_i^t$ ,  $r \in \{0, 1\}$ . Knowing that EM algorithm is sensitive to initialization, with the prior knowledge that most of the clients in  $S_i^t$  are same-cluster (it is also possible that it includes outliers), so we can initialize a better parameter as

$$\gamma_{j,r}^{(1)} = \begin{cases} 1, & j \in S_i^t \text{ and } r = 1, \text{ or } j \in C_i^t \text{ and } r = 0 \\ 0, & \text{otherwise.} \end{cases}$$

While the latent variable is the distribution parameters:  $\Theta_0 = (\mu_0, \sigma_0)$ ,  $\Theta_1 = (\mu_1, \sigma_1)$ , so the complete data is

$$(y_j, \Theta_0, \Theta_1), j \in M_i^t.$$

Then we formulate the expectation function  $Q$ , based on the log likelihood function of complete data,

$$\begin{aligned} Q(\gamma, \gamma^{(a)}) &= \mathbb{E}[\log \Pr(y, \Theta|\gamma)|y, \gamma^{(a)}] \\ &= \sum_{r=0}^1 \left\{ n_r \log \mathbb{E}\beta_r + \sum_{j \in M_i^t} \gamma_{j,r} \left[ \log\left(\frac{1}{\sqrt{2\pi}}\right) - \log \mathbb{E}\sigma_r \right. \right. \\ &\quad \left. \left. - \frac{1}{2\mathbb{E}\sigma_r^2} (y_j - \mathbb{E}\mu_r)^2 \right] \right\}, \end{aligned} \quad (15)$$

where  $n_r = \sum_{j \in M_i^t} \gamma_{j,r}$ .

**E-step:** Now we need to estimate  $\mathbb{E}(\mu_r, \sigma_r, \beta_r)$ , notated as  $\hat{\mu}_r, \hat{\sigma}_r, \hat{\beta}_r$ .

$$\hat{\mu}_r = \frac{\sum_{j \in M_i^t} \gamma_{j,r} y_j}{n_r}, \hat{\beta}_r = \frac{n_r}{|M_i^t|}, \hat{\sigma}_r^2 = \frac{\sum_{j \in M_i^t} \gamma_{j,r} (y_j - \hat{\mu}_r)^2}{n_r},$$

where  $r \in \{0, 1\}$ .

**M-step:** Iterative M-step is to find the maximum of the function  $Q(\gamma, \gamma^{(a)})$  with respect to  $\gamma^{(a)}$ , as to set  $\gamma^{(a+1)}$  in the next iterative epoch

$$\gamma^{(a+1)} = \arg \max_{\gamma} Q(\gamma, \gamma^{(a)}). \quad (16)$$

We use the following function to maximize expectation, since  $y_j$  more likely belongs to  $\mathcal{N}_0$  if  $\beta_0 \phi(y_j|\Theta_0) > \beta_1 \phi(y_j|\Theta_1)$ , vice versa

$$\gamma_{j,r}^{(a+1)} = \mathbb{I} \left\{ r = \arg \max_r \frac{\hat{\beta}_r \phi(y_j|\hat{\Theta}_r)}{\sum_{c=0}^1 \hat{\beta}_c \phi(y_j|\hat{\Theta}_c)} \right\} \quad (17)$$

$$j \in M_i^t, r \in \{0, 1\}.$$

Repeat the E-step and M-step until  $\gamma^{(a+1)} = \gamma^{(a)}$ . Then we obtain the estimated same-cluster neighbors in this round notated as  $H_i^t$ , where  $\gamma_{j,0} = 1$ ,  $j \in H_i^t$ ,  $H_i^t \subseteq M_i^t$ , then we update our neighbor list

$$N_i^{t+1} = (N_i^t - S_i^t) \cup H_i^t. \quad (18)$$

By HNM algorithm, clients can continually update their neighbors, adding new same-cluster clients and removing outliers in neighbor list.

### 3.2.4 PANM: Personalized Adaptive Neighbor Matching

Now we present PANM by combining the above-mentioned algorithms. First, in stage one, client  $i$  ( $i \in \{1, \dots, n\}$ ) communicates randomly in the network while conducting confident neighbor initialization for  $T_1$  rounds. The neighbor list  $N_i^t$  in the last round of stage one is set as the initial neighbor list in stage two. Second, in stage two, client  $i$  operates gossip communications with neighbors sampled from  $N_i^t$  for aggregation and performs heuristic neighbor matching every  $\tau$  rounds for updating the neighbor list. The process of PANM is shown in Algorithm 1. To improve readability, we summarize our main notations used in PANM as in Table 1.

TABLE 1: Important notations in this paper.

Notation	Meaning
$i$	Client $i$
$n$	Number of all clients
$a$	Number of clients in the same cluster as client $i$
$k$	Size of aggregation neighbors
$l$	Size of neighbor candidate list
$\tau$	Round interval of HNM in stage two
$\alpha$	Hyperparameter in gradient-based metric
$N_i^t$	Neighbor list of client $i$ in round $t$
$C_i^t$	Neighbor candidate list of client $i$ in round $t$
$S_i^t$	Selected neighbor in EM-step
$M_i^t$	Union set of $C_i^t$ and $S_i^t$
$H_i^t$	Neighbor estimation list in EM-step of client $i$

---

**Algorithm 1** PANM: Personalized Adaptive neighbor Matching

---

**Input:**  $n, k, l, T_1, T_2, \eta, e, \tau, \alpha, \mathbf{w}_0, \mathbf{W}^1 = \{\mathbf{w}_i^1 = \mathbf{w}_0, i \in \{1, \dots, n\}\}$ ;

**Output:**  $\mathbf{W}^{T_1+T_2}, N$ ;

```

1: Initiate neighbor list:  $N_i$ ;
2: for each round  $t = 1, \dots, T_1 + T_2$  do
3:   for each client  $i, i \in \{1, \dots, n\}$  in parallel do
4:     Compute  $e$  epochs of local training:
5:      $\mathbf{w}_i^t \leftarrow \mathbf{w}_i^t - \eta \nabla F_i(\mathbf{w}_i^t, \xi_i), \xi_i \sim \mathcal{D}_i$ ;
6:     if  $t \in \{1, \dots, T_1\}$  then
7:        $N_i^{t+1} \leftarrow \text{ConfiNeighInit}(N_i^t)$ ,
8:        $\mathbf{w}_i^{t+1} \leftarrow \text{Aggregation}(N_i^{t+1}, \mathbf{w}_i^t)$ ;
9:     else
10:      if  $t \% \tau = 0$  then
11:         $N_i^{t+1} \leftarrow \text{HeurNeighMatch}(N_i^t)$ ,
12:         $\mathbf{w}_i^{t+1} \leftarrow \text{GossipAggre}(N_i^{t+1}, \mathbf{w}_i^t)$ ;
13:      else
14:         $N_i^{t+1} \leftarrow N_i^t$ ,
15:         $\mathbf{w}_i^{t+1} \leftarrow \text{GossipAggre}(N_i^{t+1}, \mathbf{w}_i^t)$ ;
16:      end if
17:    end if
18:  end for
19: end for

```

---

## 4 EXPERIMENTS AND RESULTS

In this section, we evaluate our methods and compare them with baselines. P2P FL baselines include PENS [29] (state-of-the-art personalized P2P FL algorithm), Random (gossip with random neighbors), Local (without communication), FixTopology (neighbors are randomly sampled at the beginning and fixed during training), Oracle (with prior knowledge of cluster identities, gossip with same-cluster clients). We mention that Oracle is the ideal scenario with ground-truth cluster information which is not realistic in practices, but the following experiments will show our methods can sometimes surpass it.

Centralized FL baselines include IFCA [9] (state-of-the-art centralized clustered FL) and centralized Federated Averaging [1]. Our methods include PANMLoss (PANM with metric based on loss), PANMGrad (PANM with metric based on weight updates and gradients).

### 4.1 Settings of Datasets

We use three public benchmark datasets, MNIST [31], CIFAR10 [32], and FMNIST (Fashion-MNIST) [33]. To generate clustered Non-IID data, we use rotation transformation and label-swapping, respectively; we note these two Non-IID settings are commonly used in clustered FL (rotation [9], [29], label-swapping [11]). All results are evaluated on each client's local testset, we keep the size of local testset to 100 for all scenarios and present the averaged results among all clients. As detailed below, we describe how we prepare the Non-IID data settings for MNIST, FMNIST, and CIFAR10.

**Rotation Transformation:** There are two settings for rotation transformation. First is rotation with two clusters ( $\{0^\circ, 180^\circ\}$ ): clients in cluster 0 keep images without any transformation ( $0^\circ$  rotation) while clients in cluster 1 rotate every image in trainset and testset for  $180^\circ$ . Second is rotation with four clusters ( $\{0^\circ, 90^\circ, 180^\circ, 270^\circ\}$ ): client in cluster 0 keep images without any transformation ( $0^\circ$  rotation), clients in cluster 1 rotate every image in trainset and testset for  $90^\circ$ , clients in cluster 2 for  $180^\circ$ , and clients in cluster 3 for  $270^\circ$ . The labels of images keep unchanged and we state that the class distributions in each client are balanced.

**Swapping Labels:** There are two settings for swapping labels. First is forming two clusters by swapping labels: for clients in cluster 0, images labeled as "0" are relabeled as "1" and images labeled as "1" are relabeled as "0"; while for clients in cluster 1, images labeled as "6" are relabeled as "7" and images labeled as "7" are relabeled as "6". Second is forming four clusters by swapping labels: (1) for clients in cluster 0, images labeled as "0" and "1" are swapped by labels; (2) for clients in cluster 1, images labeled as "2" and "3" are swapped; (3) for clients in cluster 2, images labeled as "4" and "5" are swapped; (4) for clients in cluster 3, images labeled as "6" and "7" are swapped. Note that the class distributions in each client are balanced.

### 4.2 Details of Implementations

All the experiments are implemented in PyTorch 1.7.1. We have several GPUs for training, including Tesla P40 GPU with 24451MB memory, Quadro RTX 8000 GPU with 48601MB memory, Tesla P100 GPU with 16280MB memory, and Tesla V100 GPU with 16130MB memory. For all experiments, we set the batch size to 128 and the number of local epochs in each round is 3. We adopt the learning rate decay strategy used in the literature. The decay step size is 0.99, which means for each round, the learning rate is set to *the learning rate in the last round*  $\times 0.99$ . This strategy is adopted in the former work of cluster FL [9]. The initial learning rate is set to 0.08 in the first round. We use the SGD optimizer and set SGD momentum to 0.9. In every setting, we conduct experiments with different random initialization 3 times and averages the results, the mean results and the standard deviations are shown in the tables and figures. We set  $T_1 = 100$ ,  $T_2 = 200$  in all experiments.

A three-layer MLP with ReLU activations is adopted as the model for training on MNIST and FMNIST, the first layer is (28\*28, 200), the second is (200, 200), and the last is (200, 10). For CIFAR10, a convolution neural network model with ReLU activations which consists of 3 convolutional layers followed by 2 fully connected layers is used. We do not use

any image preprocessing transformation, such as flipping and random cropping.

For “the expected amount of times” in PENS, we set this hyperparameter to an appropriate value ( $\text{ceil}(T_1 \times (l+k)/n)$ ) for fair comparison. For centralized FL: IFCA and FedAvg, we set full participation of clients in each round of federated training.

### 4.3 Results on Different Datasets

Table 2 shows the accuracies of all methods being compared under different datasets. Although fixed topology and random gossip improve accuracy compared with local training, in contrast to Oracle, the fixed and random topology will impede performance gains. Note that Oracle is with perfect information about cluster identities which is impossible in real FL scenarios, however, our methods surpass Oracle in FMNIST and CIFAR10. We show accuracy and loss curves of results in CIFAR10 in Figure 6, it is demonstrated that PANM (especially PANMLoss) achieves high accuracies in stage one, which means the CNI algorithm is effective, also, PANM converges faster than others. We explain that CNI not only makes sure the neighbors are confident to be same-cluster, it also enables collaboration with neighbors that have maximum similarities among all seen clients, so the performance will be better than randomly sampled from same-cluster peers (Oracle). In Figure 5, we illustrate the heatmaps of aggregation records between clients in stage one, from which we can see: PENS has noisy aggregations while clients in PANM only aggregates with same-cluster clients; in PANM, clients are prone to communicate with several maximum-similarity clients, the directional communications help PANM to reach better performance. Additionally, we notice that PENS performs better in easy datasets like MNIST, because the objective discrepancy between clusters is not dominant, introducing different-cluster neighbors will not do much harm to local performance.

TABLE 2: Results on different datasets. The top two are in bold. For all datasets: trainset size is 200, two rotations  $\{0^\circ, 180^\circ\}$ ,  $l = 10, k = 5$ .  $n = 100$  for CIFAR10 and FMNIST,  $n = 200$  for MNIST.

Methods	MNIST	FMNIST	CIFAR10
Local	82.57 $\pm$ 0.28	76.24 $\pm$ 0.22	25.27 $\pm$ 1.21
FixTopology	94.71 $\pm$ 0.09	85.86 $\pm$ 0.17	39.74 $\pm$ 2.27
Random	95.12 $\pm$ 0.04	85.94 $\pm$ 0.27	42.96 $\pm$ 1.42
Oracle	<b>95.87 <math>\pm</math> 0.08</b>	<b>87.01 <math>\pm</math> 0.26</b>	<b>49.11 <math>\pm</math> 0.48</b>
PENS	<b>96.15 <math>\pm</math> 0.16</b>	86.82 $\pm$ 0.11	44.78 $\pm$ 1.12
PANMLoss	95.63 $\pm$ 0.12	<b>87.33 <math>\pm</math> 0.17</b>	<b>49.19 <math>\pm</math> 0.79</b>
PANMGrad	95.65 $\pm$ 0.09	86.88 $\pm$ 0.34	48.83 $\pm$ 0.39

### 4.4 Results under Various Heterogeneity

Table 3 shows results under various heterogeneity: randomly swapping out labels and more rotations. For accuracy, it is obvious that our methods are robust in different Non-IID environments. It is notable that in some experiments (CIFAR10 Label-swap(2)(4)), PANM even outperforms Oracle with a large margin. Overall, PANMGrad

TABLE 3: Results under various heterogeneity. CIFAR10,  $n = 100, l = 10, k = 5$ , trainset size is 200. Label-swap(2)/(4): two/four clusters with swapping labels, Rotation(4): four clusters with rotation  $\{0^\circ, 90^\circ, 180^\circ, 270^\circ\}$ .

Test Accuracy			
Methods	Label-swap(2)	Label-swap(4)	Rotation(4)
Local	25.27 $\pm$ 1.21	25.27 $\pm$ 1.21	25.27 $\pm$ 1.21
FixTopology	36.56 $\pm$ 1.58	35.08 $\pm$ 2.70	31.86 $\pm$ 0.47
Random	37.32 $\pm$ 0.26	37.14 $\pm$ 1.30	33.16 $\pm$ 0.55
Oracle	43.34 $\pm$ 1.29	43.32 $\pm$ 1.06	<b>43.32 <math>\pm</math> 0.85</b>
PENS	45.72 $\pm$ 1.34	<b>43.49 <math>\pm</math> 0.28</b>	36.64 $\pm$ 0.58
PANMLoss	<b>47.12 <math>\pm</math> 1.30</b>	<b>45.78 <math>\pm</math> 1.85</b>	41.43 $\pm$ 1.83
PANMGrad	<b>45.84 <math>\pm</math> 1.92</b>	42.14 $\pm$ 1.34	<b>43.99 <math>\pm</math> 1.26</b>
Precision of Neighbors			
Methods	Label-swap(2)	Label-swap(4)	Rotation(4)
PENS	<b>100</b>	70.83 $\pm$ 4.17	59.75 $\pm$ 5.08
PANMLoss	<b>100</b>	<b>100</b>	68.19 $\pm$ 28.12
PANMGrad	<b>100</b>	83.33 $\pm$ 28.87	<b>100</b>
Recall of Neighbors			
Methods	Label-swap(2)	Label-swap(4)	Rotation(4)
PENS	59.18 $\pm$ 2.04	66.67 $\pm$ 4.17	52.78 $\pm$ 8.67
PANMLoss	74.15 $\pm$ 32.42	48.61 $\pm$ 13.39	62.50 $\pm$ 31.46
PANMGrad	<b>100</b>	<b>94.44 <math>\pm</math> 6.36</b>	<b>98.61 <math>\pm</math> 2.41</b>

has similar performances to PANMLoss, but performances vary regarding different settings. This is due to the different perspectives on understanding client similarity, one is based on training loss, another is based on consistency of gradient updates; the two perspectives will take advantage in different scenarios.

For precision (the fraction of same-cluster clients among neighbors) and recall (the fraction of same-cluster neighbors among all same-cluster clients) in stage two, our methods outperform PENS, which means our EM-based heuristic neighbor matching method is effective to enable clients to match most of the same-cluster clients as neighbors. We also demonstrate the neighbor topologies of PANMLoss and PENS in stage two in Figure 7, by PANM, clients evolve to form the four-cluster structure without prior knowledge of cluster identities, whereas PENS constructs a disordered topology.

### 4.5 Impact of Trainset size and Number of Clients

In the left figure of Figure 8, we compare PANM to the baselines in a setting where we fix the number of clients to 100 while varying the size of the local trainsets. The results show that by increasing the size of the local train set on each client, performance increases for all compared algorithms. We further see that PANM consistently outperforms all baselines (including PENS), and it has comparable performance to Oracle, especially when the trainset size is large. Compared with PENS, PANM surpasses it with a large margin, especially in scenarios where data are sufficient.

In the right figure of Figure 8, results of changing number of clients are shown, in this experiment, we fix the trainset size to 200. Overall, performances increase while adding



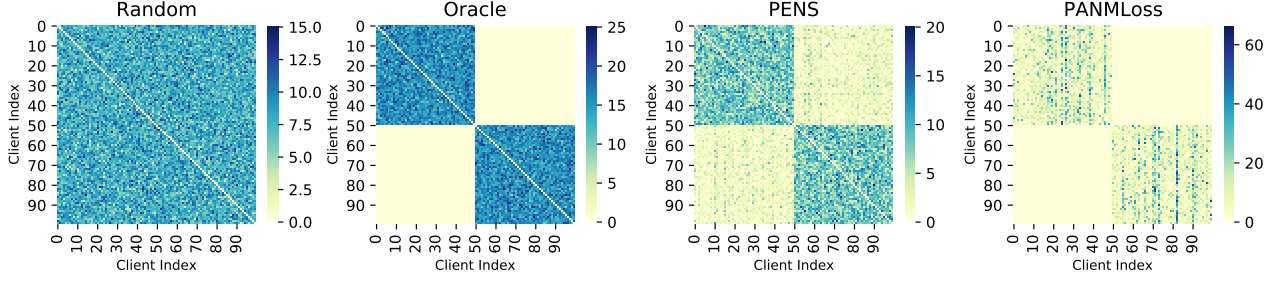


Fig. 5: Heatmaps of aggregation records in stage one. CIFAR-10 with two rotations  $\{0^\circ$ : clients 0-49,  $180^\circ$ : clients 50-99 $\}$ , trainset size is 400,  $l = 10$ ,  $k = 5$ .

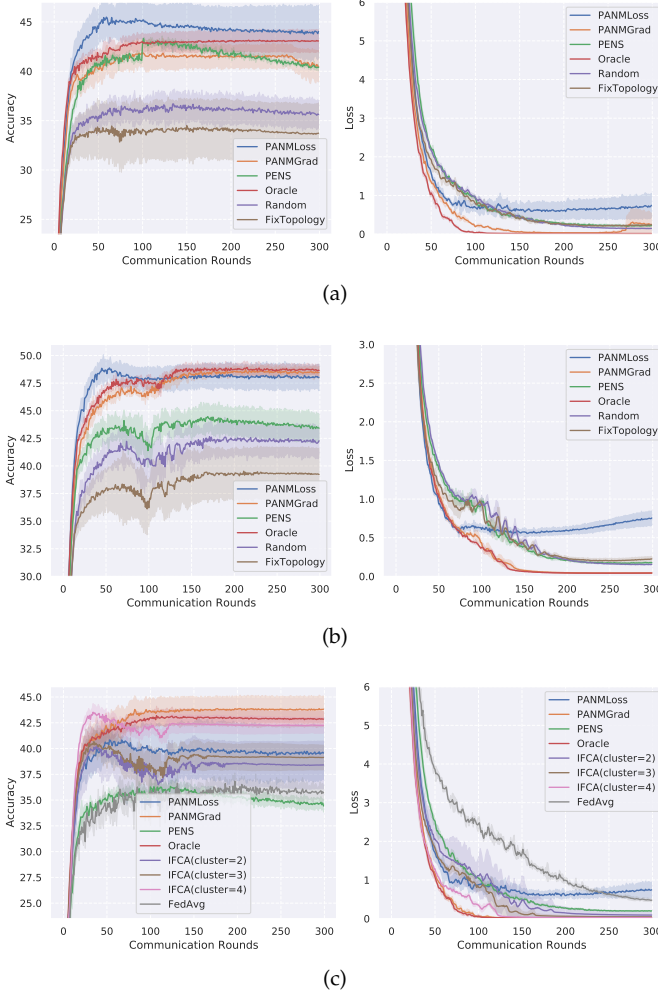


Fig. 6: Accuracy and loss curves. CIFAR10,  $n = 100$ ,  $l = 10$ ,  $k = 5$ , trainset size is 200. (a) 4 clusters with swapping labels; (b) 2 clusters with rotations  $\{0^\circ, 180^\circ\}$ ; (c) comparing with centralized FL methods, 4 clusters with rotations  $\{0^\circ, 90^\circ, 180^\circ, 270^\circ\}$ .

more clients for participation, and PANM outperforms all baselines in all settings. However, when the number of clients is large, PANM may have inferior performance to Oracle, but it is also superior compared with others.

#### 4.6 Impact of $l$ and $k$

$l$  is the number of randomly sampled neighbor candidates, and  $k$  is the number of neighbors for aggregation chosen from neighbor candidates or the neighbor list. The choices of  $l$  and  $k$  depend on communication budgets in the system, larger  $l$  and  $k$  will bring more communication costs. Besides, the ratio of  $l$  and  $k$  is also crucial (especially for PENS), it decides the probabilities of neighbors being same-cluster as we have inferred in Theorem 1 and Corollary 1. We conduct experiments by changing  $l$ ,  $k$  as demonstrated in Table 4.

We notice that in easy settings (for example,  $l = 10$ ,  $k = 3$ ), PENS performs well, but in other settings, PENS has poor results. As we discussed in the paper, if the setting is difficult, PENS is prone to be noisy in neighbor matching.

For oracle, only  $k$  matters, because  $k$  determines the number of neighbors to collaborate with in each round. As  $k$  increases, performances of Oracle also increase. We explain that if the number of neighbors for aggregation increases, it is better for clients to reach partial consensus within clusters, and the model weights are more likely to be similar. It is worth mentioning that PANMLoss is very robust, and it surpasses Oracle in most settings. PANMLoss benefits a lot when  $k$  increases.

#### 4.7 Comparison with Centralized Clustered FL

P2P FL takes advantage of bandwidth and reliability as we addressed in Section 1; besides, as for clustered FL, P2P solutions are more robust and can exploit the latent cluster structure in a self-evolved manner without assuming the number of clusters. We compare IFCA [9], the present state-of-the-art centralized clustered FL and centralized Federated Averaging [1] with decentralized P2P methods, as shown in Table 5 and (c) of Figure 6. In typical centralized FL algorithms, the central server randomly samples  $l$  clients for aggregation, but we notice that this will result in bad convergence for IFCA. In our implementations, in a scenario where there are 100 clients with 4 clusters therein, and the central server samples 10 clients in each round (where  $l/n = 0.1$ ), IFCA has poor convergence of estimations: all clients are estimated as the same identity. As a result, we have to set full aggregation participation of clients in IFCA, but we remind this will cause large communication burdens and it is unfair to the P2P setting (where we set  $n = 100$ ,  $l = 10$ ,  $l/n = 0.1$ ). Even if, in Table 5, our P2P method PANM also achieves proportionate performances as a contrast to IFCA. What's more, IFCA requires assumptions

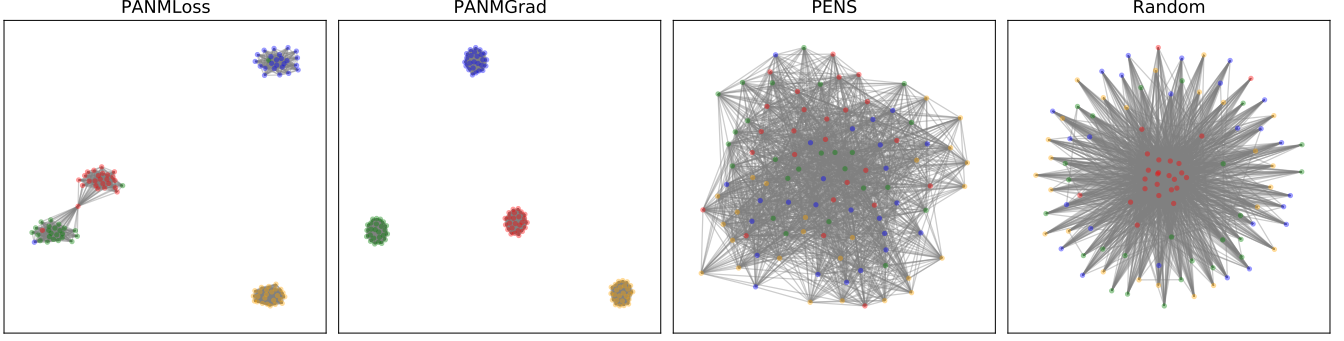


Fig. 7: Neighbor topologies in stage two. Four clusters with rotations, CIFAR10,  $n = 100$ ,  $l = 10$ ,  $n = 5$ , trainset size is 200. Each color denotes a cluster.

TABLE 4: Impact of  $k$  and  $l$ . CIFAR10 with two rotations  $\{0^\circ, 180^\circ\}$ ,  $n = 100$ , trainset size is 100 for all settings.

Methods	$l, k$					
	10,5	10,3	20,10	20,5	30,15	30,10
Local	19.93 $\pm$ 0.36	19.93 $\pm$ 0.36	19.93 $\pm$ 0.36	19.93 $\pm$ 0.36	19.93 $\pm$ 0.36	19.93 $\pm$ 0.36
FixTopology	36.60 $\pm$ 2.58	31.54 $\pm$ 0.18	38.31 $\pm$ 1.45	34.94 $\pm$ 0.84	38.88 $\pm$ 0.52	38.77 $\pm$ 3.80
Random	39.19 $\pm$ 1.04	38.54 $\pm$ 2.24	40.82 $\pm$ 1.09	37.34 $\pm$ 0.80	42.22 $\pm$ 2.25	39.91 $\pm$ 0.60
Oracle	<b>43.83 <math>\pm</math> 0.80</b>	<b>42.28 <math>\pm</math> 1.25</b>	<b>43.39 <math>\pm</math> 2.80</b>	<b>43.57 <math>\pm</math> 0.93</b>	<b>44.79 <math>\pm</math> 2.36</b>	<b>44.16 <math>\pm</math> 1.32</b>
PENS	42.42 $\pm$ 1.58	<b>40.04 <math>\pm</math> 0.90</b>	42.57 $\pm$ 1.74	41.92 $\pm$ 1.28	44.12 $\pm$ 0.22	42.80 $\pm$ 0.98
PANMLoss	41.75 $\pm$ 0.24	39.55 $\pm$ 1.78	<b>44.02 <math>\pm</math> 0.59</b>	<b>43.64 <math>\pm</math> 1.54</b>	<b>46.82 <math>\pm</math> 0.41</b>	<b>46.19 <math>\pm</math> 0.84</b>
PANMGrad	<b>42.48 <math>\pm</math> 0.21</b>	39.53 $\pm$ 2.99	38.24 $\pm$ 4.26	41.94 $\pm$ 3.15	41.16 $\pm$ 3.60	42.23 $\pm$ 1.02

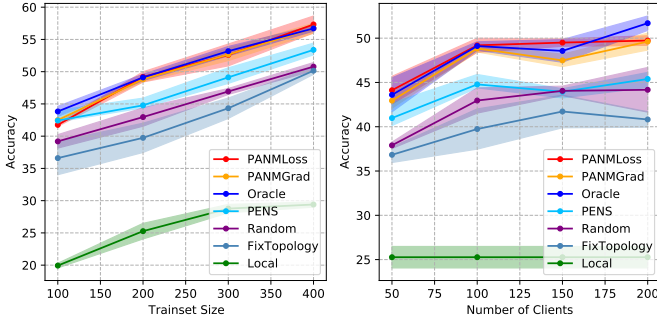


Fig. 8: Left: Accuracies when changing trainset size;  $n = 100$ ,  $l = 10$ ,  $k = 5$ , two rotations  $\{0^\circ, 180^\circ\}$  for all. Right: Accuracies when changing number of clients,  $l = 10$ ,  $k = 5$ , trainset size is 200, two rotations  $\{0^\circ, 180^\circ\}$  for all.

on the number of clusters ( $c$ ), we find: if  $c$  is set inappropriately, the performance will be poor. According to Table 5, in scenario of CIFAR10 with 4 rotations, if set  $c = 2$ , the accuracy of IFCA is 40.64% while our PANMLoss and PANMGrad reach 41.43% and 43.99%. Moreover, from the learning curves in Figure (c) of Figure 6, it is apparent that our P2P methods PANM keeps a more steady and robust learning process while there are some disturbances in the curves of centralized counterparts and our P2P solutions have the same convergence rate with the centralized ones.

We notice that, generally, the overall communication costs of P2P FL are larger than those of centralized FL methods, since every client needs to receive and transmit several models in a communication round. Hence, we implement PANM under low communication budgets so that PANM

TABLE 5: Comparing with centralized FL.  $n = 100$ ,  $l = 10$ ,  $k = 5$ , trainset size is 200. Best performances in the centralized and decentralized are in bold. Clusters are generated by rotations: 2 for  $\{0^\circ, 180^\circ\}$ , 4 for  $\{0^\circ, 90^\circ, 180^\circ, 270^\circ\}$ .

Methods	CIFAR10(4)	FMNIST(4)	FMNIST(2)
Local	25.27 $\pm$ 1.21	76.24 $\pm$ 0.22	76.24 $\pm$ 0.22
FedAvg	37.03 $\pm$ 0.74	83.54 $\pm$ 0.08	86.86 $\pm$ 0.16
IFCA( $c=2$ )	40.64 $\pm$ 2.18	86.19 $\pm$ 0.04	<b>88.06 <math>\pm</math> 0.20</b>
IFCA( $c=3$ )	41.05 $\pm$ 1.09	<b>86.78 <math>\pm</math> 0.36</b>	/
IFCA( $c=4$ )	<b>43.65 <math>\pm</math> 0.77</b>	86.50 $\pm$ 0.07	/
Oracle	43.32 $\pm$ 0.85	85.45 $\pm$ 0.38	87.01 $\pm$ 0.26
PENS	36.64 $\pm$ 0.58	84.68 $\pm$ 0.27	86.82 $\pm$ 0.11
PANMLoss	41.43 $\pm$ 1.83	<b>86.09 <math>\pm</math> 0.31</b>	<b>87.33 <math>\pm</math> 0.17</b>
PANMGrad	<b>43.99 <math>\pm</math> 1.26</b>	85.64 $\pm$ 0.25	86.88 $\pm$ 0.34

TABLE 6: Performances under low communication budgets, where  $n = 100$ , the trainset size is 200 and  $\Delta = 100\delta$  with  $\delta$  being the single model size. We use CIFAR-10 with 4 rotations. For PANM, we set  $l = 4$ ,  $\tau = 10$ .

Methods	Comm. costs	Max. req. band.	Test acc.
FedAvg	600 $\Delta$	1 $\Delta$	37.03 $\pm$ 0.74
IFCA ( $c=2$ )	900 $\Delta$	2 $\Delta$	40.64 $\pm$ 2.18
IFCA ( $c=3$ )	1200 $\Delta$	3 $\Delta$	41.05 $\pm$ 1.09
IFCA ( $c=4$ )	1500 $\Delta$	4 $\Delta$	<b>43.65 <math>\pm</math> 0.77</b>
PANMLoss ( $k=2$ )	1118 $\Delta$	0.06 $\Delta$	41.36 $\pm$ 0.64
PANMGrad ( $k=2$ )	1118 $\Delta$	0.06 $\Delta$	42.78 $\pm$ 1.68
PANMLoss ( $k=3$ )	1397 $\Delta$	0.07 $\Delta$	43.30 $\pm$ 1.32
PANMGrad ( $k=3$ )	1397 $\Delta$	0.07 $\Delta$	<b>43.34 <math>\pm</math> 0.85</b>

will have comparable overall communication costs as the

centralized, and we conclude the results in Table 6. It shows that PANM can have close performances to IFCA when the communication costs are similar but PANM requires much lower bandwidth. We also find that the consequence of inappropriately estimating the number of clusters will be severe for IFCA ( $c = 4$  : 43.65;  $c = 3$  : 41.05), but PANM is flexible enough to explore the cluster structure under any hyperparameters. The influence of communication budgets is subtle for PANM, therefore it is more robust and effective than the centralized IFCA.

## 5 DISCUSSION

### 5.1 Performance of PANMLoss and PANMGrad

For simple datasets (e.g. MNIST), we observed that the performance of the two algorithms is comparable. As for CIFAR-10, PANMLoss performs better in rotation (2) and label-swap, while PANMGrad performs better in rotation (4). We explain this by the inter-cluster objective inconsistency (IOI). If IOI is dominant, which means that the learning tasks are diverse, thus the losses are distinct and PANMLoss will be beneficial. We consider the IOI as: label-swap > rotation, rotation (2) > rotation (4). However, when IOI is low, the loss-based metric is noisy, the proposed PANMGrad will exploit two cosine functions to provide a more accurate similarity measurement.

Additionally, we notice in Figure 3 that PANMGrad will result in faster convergence of precision of same-cluster neighbors which means the metric based on gradients is more effective in the early stage of training.

### 5.2 Applicability of PANM

For PANMLoss and PANMGrad, the metrics require different computation resources. Generally, PANMGrad is more computationally efficient, since it only requires several inner product calculations on sparse vectors (gradients), while PANMLoss needs inference on local datasets. Hence, under limited computation resources, PANMGrad is more preferable. In addition, as we mentioned before, if IOI is high, PANMLoss is more suggested, otherwise, PANMGrad may be better.

We have mentioned in Subsection 4.6 that we can choose different  $l, k$  by the communication budgets and we have shown PANM is still effective under low communication budgets. Furthermore, in our implementations, we assume fully connected communication accessibility, which means that each client is able to communicate with any other client in the system. The fully connected accessibility is not often satisfied in realistic scenarios, but we state that PANM is also applicable under limited accessibility. In PANM, we make loose assumption on accessibility, clients can purify their neighbors within the scope of accessible peers. Thus, PANM is flexible in practice.

## 6 CONCLUSION

In this paper, we study the clustered Non-IID problem in peer-to-peer federated learning and develop PANM that enables clients to match neighbors with similar objectives. We analyze how PANM works, and empirically demonstrate that it significantly improves the performance compared with strong baselines.

## REFERENCES

- [1] B. McMahan, E. Moore, D. Ramage, S. Hampson, and B. A. y Arcas, "Communication-efficient learning of deep networks from decentralized data," in *Proceedings of the 20th International Conference on Artificial Intelligence and Statistics, AISTATS 2017, 20-22 April 2017, Fort Lauderdale, FL, USA*, ser. Proceedings of Machine Learning Research, A. Singh and X. J. Zhu, Eds., vol. 54. PMLR, 2017, pp. 1273–1282. [Online]. Available: <http://proceedings.mlr.press/v54/mcmahan17a.html>
- [2] Q. Yang, Y. Liu, T. Chen, and Y. Tong, "Federated machine learning: Concept and applications," *ACM Trans. Intell. Syst. Technol.*, vol. 10, no. 2, pp. 12:1–12:19, 2019. [Online]. Available: <https://doi.org/10.1145/3298981>
- [3] T. Li, A. K. Sahu, A. Talwalkar, and V. Smith, "Federated learning: Challenges, methods, and future directions," *IEEE Signal Process. Mag.*, vol. 37, no. 3, pp. 50–60, 2020. [Online]. Available: <https://doi.org/10.1109/MSP.2020.2975749>
- [4] P. Kairouz, H. B. McMahan, B. Avent, A. Bellet, M. Bennis, A. N. Bhagoji, K. A. Bonawitz, Z. Charles, G. Cormode, R. Cummings, R. G. L. D'Oliveira, H. Eichner, S. E. Rouayheb, D. Evans, J. Gardner, Z. Garrett, A. Gascón, B. Ghazi, P. B. Gibbons, M. Gruteser, Z. Harchaoui, C. He, L. He, Z. Huo, B. Hutchinson, J. Hsu, M. Jaggi, T. Javidi, G. Joshi, M. Khodak, J. Konečný, A. Korolova, F. Koushanfar, S. Koyejo, T. Lepoint, Y. Liu, P. Mittal, M. Mohri, R. Nock, A. Özgür, R. Pagh, H. Qi, D. Ramage, R. Raskar, M. Raykova, D. Song, W. Song, S. U. Stich, Z. Sun, A. T. Suresh, F. Tramèr, P. Vepakomma, J. Wang, L. Xiong, Z. Xu, Q. Yang, F. X. Yu, H. Yu, and S. Zhao, "Advances and open problems in federated learning," *Found. Trends Mach. Learn.*, vol. 14, no. 1-2, pp. 1–210, 2021. [Online]. Available: <https://doi.org/10.1561/22000000083>
- [5] Y. Li, X. Liu, X. Zhang, Y. Shao, Q. Wang, and Y. Geng, "Personalized federated learning via maximizing correlation with sparse and hierarchical extensions," *arXiv preprint arXiv:2107.05330*, 2021.
- [6] H. Zhu, J. Xu, S. Liu, and Y. Jin, "Federated learning on non-iid data: A survey," *CoRR*, vol. abs/2106.06843, 2021. [Online]. Available: <https://arxiv.org/abs/2106.06843>
- [7] B. M. Sarwar, G. Karypis, J. Konstan, and J. Riedl, "Recommender systems for large-scale e-commerce: Scalable neighborhood formation using clustering," in *Proceedings of the fifth international conference on computer and information technology*, vol. 1. Citeseer, 2002, pp. 291–324.
- [8] Q. Li and B. M. Kim, "Clustering approach for hybrid recommender system," in *Proceedings IEEE/WIC International Conference on Web Intelligence (WI 2003)*. IEEE, 2003, pp. 33–38.
- [9] A. Ghosh, J. Chung, D. Yin, and K. Ramchandran, "An efficient framework for clustered federated learning," in *Advances in Neural Information Processing Systems 33: Annual Conference on Neural Information Processing Systems 2020, NeurIPS 2020, December 6-12, 2020, virtual*, H. Larochelle, M. Ranzato, R. Hadsell, M. Balcan, and H. Lin, Eds., 2020. [Online]. Available: <https://proceedings.neurips.cc/paper/2020/hash/e32cc80bf07915058ce90722ee17bb71-Abstract.html>
- [10] M. Xie, G. Long, T. Zhou, X. Wang, and J. Jiang, "Multi-center federated learning," *CoRR*, vol. abs/2005.01026, 2020. [Online]. Available: <https://arxiv.org/abs/2005.01026>
- [11] F. Sattler, K. Müller, and W. Samek, "Clustered federated learning: Model-agnostic distributed multitask optimization under privacy constraints," *IEEE Trans. Neural Networks Learn. Syst.*, vol. 32, no. 8, pp. 3710–3722, 2021. [Online]. Available: <https://doi.org/10.1109/TNNLS.2020.3015958>
- [12] M. Duan, D. Liu, X. Ji, Y. Wu, L. Liang, X. Chen, Y. Tan, and A. Ren, "Flexible clustered federated learning for client-level data distribution shift," *IEEE Transactions on Parallel and Distributed Systems*, 2021.
- [13] X. Lian, C. Zhang, H. Zhang, C. Hsieh, W. Zhang, and J. Liu, "Can decentralized algorithms outperform centralized algorithms? A case study for decentralized parallel stochastic gradient descent," in *Advances in Neural Information Processing Systems 30: Annual Conference on Neural Information Processing Systems 2017, December 4-9, 2017, Long Beach, CA, USA*, I. Guyon, U. von Luxburg, S. Bengio, H. M. Wallach, R. Fergus, S. V. N. Vishwanathan, and R. Garnett, Eds., 2017, pp. 5330–5340. [Online]. Available: <https://proceedings.neurips.cc/paper/2017/hash/f75526659f31040af6b61cb7133e4e6d-Abstract.html>

- [14] A. Lalitha, O. C. Kilinc, T. Javidi, and F. Koushanfar, "Peer-to-peer federated learning on graphs," *CoRR*, vol. abs/1901.11173, 2019. [Online]. Available: <http://arxiv.org/abs/1901.11173>
- [15] A. Lalitha, S. Shekhar, T. Javidi, and F. Koushanfar, "Fully decentralized federated learning," in *Third workshop on Bayesian Deep Learning (NeurIPS)*, 2018.
- [16] T. Lin, S. P. Karimireddy, S. U. Stich, and M. Jaggi, "Quasi-global momentum: Accelerating decentralized deep learning on heterogeneous data," in *Proceedings of the 38th International Conference on Machine Learning, ICML 2021, 18-24 July 2021, Virtual Event*, ser. Proceedings of Machine Learning Research, M. Meila and T. Zhang, Eds., vol. 139. PMLR, 2021, pp. 6654–6665. [Online]. Available: <http://proceedings.mlr.press/v139/lin21c.html>
- [17] L. Kong, T. Lin, A. Koloskova, M. Jaggi, and S. U. Stich, "Consensus control for decentralized deep learning," in *Proceedings of the 38th International Conference on Machine Learning, ICML 2021, 18-24 July 2021, Virtual Event*, ser. Proceedings of Machine Learning Research, M. Meila and T. Zhang, Eds., vol. 139. PMLR, 2021, pp. 5686–5696. [Online]. Available: <http://proceedings.mlr.press/v139/kong21a.html>
- [18] C. Briggs, Z. Fan, and P. Andras, "Federated learning with hierarchical clustering of local updates to improve training on non-iid data," in *2020 International Joint Conference on Neural Networks, IJCNN 2020, Glasgow, United Kingdom, July 19-24, 2020*. IEEE, 2020, pp. 1–9. [Online]. Available: <https://doi.org/10.1109/IJCNN48605.2020.9207469>
- [19] S. Sarkar and A. K. Ghosh, "On perfect clustering of high dimension, low sample size data," *IEEE transactions on pattern analysis and machine intelligence*, vol. 42, no. 9, pp. 2257–2272, 2019.
- [20] M. Duan, D. Liu, X. Ji, R. Liu, L. Liang, X. Chen, and Y. Tan, "Fedgroup: Ternary cosine similarity-based clustered federated learning framework toward high accuracy in heterogeneous data," *CoRR*, vol. abs/2010.06870, 2020. [Online]. Available: <https://arxiv.org/abs/2010.06870>
- [21] S. Warnat-Herresthal, H. Schultze, K. L. Shastry, S. Manamohan, S. Mukherjee, V. Garg, R. Sarveswara, K. Händler, P. Pickkers, N. A. Aziz *et al.*, "Swarm learning for decentralized and confidential clinical machine learning," *Nature*, vol. 594, no. 7862, pp. 265–270, 2021.
- [22] I. Hegedüs, G. Danner, and M. Jelasity, "Decentralized learning works: An empirical comparison of gossip learning and federated learning," *J. Parallel Distributed Comput.*, vol. 148, pp. 109–124, 2021. [Online]. Available: <https://doi.org/10.1016/j.jpdc.2020.10.006>
- [23] A. Bellet, R. Guerraoui, M. Taziki, and M. Tommasi, "Personalized and private peer-to-peer machine learning," in *International Conference on Artificial Intelligence and Statistics, AISTATS 2018, 9-11 April 2018, Playa Blanca, Lanzarote, Canary Islands, Spain*, ser. Proceedings of Machine Learning Research, A. J. Storkey and F. Pérez-Cruz, Eds., vol. 84. PMLR, 2018, pp. 473–481. [Online]. Available: <http://proceedings.mlr.press/v84/bellet18a.html>
- [24] C. Li, G. Li, and P. K. Varshney, "Decentralized federated learning via mutual knowledge transfer," *CoRR*, vol. abs/2012.13063, 2020. [Online]. Available: <https://arxiv.org/abs/2012.13063>
- [25] A. Bellet, A. Kermarrec, and E. Lavoie, "D-cliques: Compensating noniidness in decentralized federated learning with topology," *CoRR*, vol. abs/2104.07365, 2021. [Online]. Available: <https://arxiv.org/abs/2104.07365>
- [26] Z. Tang, S. Shi, and X. Chu, "Communication-efficient decentralized learning with sparsification and adaptive peer selection," in *40th IEEE International Conference on Distributed Computing Systems, ICDCS 2020, Singapore, November 29 - December 1, 2020*. IEEE, 2020, pp. 1207–1208. [Online]. Available: <https://doi.org/10.1109/ICDCS47774.2020.00153>
- [27] J. Jiang and L. Hu, "Decentralised federated learning with adaptive partial gradient aggregation," *CAAI Trans. Intell. Technol.*, vol. 5, no. 3, pp. 230–236, 2020. [Online]. Available: <https://doi.org/10.1049/trit.2020.0082>
- [28] O. Marfoq, C. Xu, G. Neglia, and R. Vidal, "Throughput-optimal topology design for cross-silo federated learning," in *Advances in Neural Information Processing Systems 33: Annual Conference on Neural Information Processing Systems 2020, NeurIPS 2020, December 6-12, 2020, virtual*, H. Larochelle, M. Ranzato, R. Hadsell, M. Balcan, and H. Lin, Eds., 2020. [Online]. Available: <https://proceedings.neurips.cc/paper/2020/hash/e29b722e35040b88678e25a1ec032a21-Abstract.html>
- [29] N. Onoszko, G. Karlsson, O. Mogren, and E. L. Zec, "Decentralized federated learning of deep neural networks on non-iid data," *CoRR*, vol. abs/2107.08517, 2021. [Online]. Available: <https://arxiv.org/abs/2107.08517>
- [30] E. Tzeng, J. Hoffman, N. Zhang, K. Saenko, and T. Darrell, "Deep domain confusion: Maximizing for domain invariance," *arXiv preprint arXiv:1412.3474*, 2014.
- [31] Y. LeCun and C. Cortes, "MNIST handwritten digit database," *arXiv*, 2010. [Online]. Available: <http://yann.lecun.com/exdb/mnist/>
- [32] A. Krizhevsky *et al.*, "Learning multiple layers of features from tiny images," *Citeseer*, 2009.
- [33] H. Xiao, K. Rasul, and R. Vollgraf, "Fashion-mnist: a novel image dataset for benchmarking machine learning algorithms," *arXiv preprint arXiv:1708.07747*, 2017.

## APPENDIX A

### PROOF OF THEOREM 1 AND COROLLARY 1

#### A.1 Proof of Theorem 1

Under Assumption 1, the similarity metrics are effective enough that all the same-cluster clients will have higher similarities than the different-cluster clients. Therefore if there are at least  $k$  same-cluster clients in the  $l$  sampled clients, the top  $k$  clients with maximum similarities must be same-cluster. As a result, we can formulate the problem of neighbors being same-cluster into the "**Ball Selection Problem**", as follows.

**Ball Selection Problem:** There are  $n - 1$  balls in the box and  $a - 1$  of them are white balls. Select  $l$  balls at one time without putting back. For the selected  $l$  balls, ask:

(1) the probability that at least  $k$  balls are white balls.

Conducting the selection for the first time and note down the number of white balls as  $s_1$ . Conducting the selection for the second time and note down the number of white balls as  $s_2$ . . . . Conducting the selection for the  $t$ -th time and note down the number of white balls as  $s_t$ . Ask:

(2) the probability that  $\sum_{c=1}^t s_c \geq k$ .

Question (1) in the "Ball Selection Problem" is equivalent to the problem that for client  $i$ , randomly sampling  $l$  clients, ask the probability that at least  $k$  clients are same-cluster. Question (2) in "Ball Selection Problem" is equivalent to the problem that for client  $i$ , conducting CNI strategy for  $t$  rounds, ask the probability that all the  $k$  neighbors in round  $t$  are same-cluster.

We further calculate the probabilities in Questions (1) and (2). We define the probability that select  $l$  balls and  $x$  of them are white balls as a function  $G(x)$  and the probability that select  $l$  balls and at least  $x$  of them are white balls as function  $R(x)$ .

First, we give the calculation of  $G(x)$ . All possible cases are: from all  $n - 1$  balls to select  $l$  balls, as  $C_{n-1}^l$ . The cases satisfying our condition are: from  $a - 1$  white balls to select  $x$  balls while from other  $n - a$  balls to select  $l - x$  balls, as  $C_{a-1}^x \cdot C_{n-a}^{l-x}$ . The equation is as follows.

$$\begin{aligned}
G(x) &= \frac{C_{a-1}^x \cdot C_{n-a}^{l-x}}{C_{n-1}^l} \\
&= \left[ \frac{(a-1)!}{x!(a-x-1)!} \cdot \frac{(n-a)!}{(l-x)!(n-a-l-x)!} \right] / \left[ \frac{(n-1)!}{l!(n-l-1)!} \right] \\
&= \frac{l!(a-1)!(n-a)!(n-l-1)!}{x!(n-1)!(l-x)!(a-x-1)!(n-a-l-x)!}.
\end{aligned} \tag{19}$$

Then, we give the calculation of  $R(x)$ . All possible cases are: from all  $n-1$  balls to select  $l$  balls, as  $C_{n-1}^l$ . The number of white balls satisfying our condition ranges from  $x$  to  $l$ , so the cases satisfying our condition are:  $x$  white balls and  $l-x$  other balls,  $x+1$  white balls and  $l-x-1$  other balls,  $\dots$ ,  $l-1$  white balls and 1 other balls,  $l$  white balls and 0 other ball. Thus the equation is as follows.

$$\begin{aligned}
R(x) &= (C_{a-1}^x \cdot C_{n-a}^{l-x} + C_{a-1}^{x+1} \cdot C_{n-a}^{l-x-1} + \dots + C_{a-1}^{l-1} \cdot C_{n-a}^1 + C_{a-1}^l \cdot C_{n-a}^0) / C_{n-1}^l \\
&= \left[ \sum_{s=0}^{l-x} \frac{(a-1)!}{(l-s)!(a-l+s-1)!} \cdot \frac{(n-a)!}{s!(n-a-s)!} \right] / \left[ \frac{(n-1)!}{l!(n-l-1)!} \right] \\
&= \frac{l!(n-l-1)!}{(n-1)!} \sum_{s=0}^{l-x} \frac{(a-1)!(n-a)!}{s!(l-s)!(n-a-s)!(a-l+s-1)!}
\end{aligned} \tag{20}$$

Obviously, for Question (1), the probability is  $P^1(k) = R(k)$ . Then, we consider the scenario where  $t = 2$  in Question (2). All the satisfying cases are: none of the white balls is selected in the first time and at least  $k$  white balls are selected in the second time, 1 white ball is selected in the first time and at least  $k-1$  white balls are selected in the second time,  $\dots$ ,  $k-1$  white balls are selected in the first time and at least 1 white balls are selected in the second time, at least  $k$  white balls are selected in the first time and it does not matter how many white balls are selected in the second time. Therefore, the equation is as follows.

$$\begin{aligned}
P^2(k) &= G(0) \cdot R(k) + G(1) \cdot R(k-1) + \dots + G(k-1) \cdot R(1) + R(k).
\end{aligned} \tag{21}$$

Similar to Equation (21), we can infer the satisfying cases when  $t = t$ : none of the white balls is selected in the first time and at least  $k$  white balls are selected in the remaining  $t-1$  times, 1 white ball is selected in the first time and at least  $k-1$  white balls are selected in the remaining  $t-1$  times,  $\dots$ ,  $k-1$  white balls are selected in the first time and at least 1 white balls are selected in the remaining  $t-1$  times, at least  $k$  white balls are selected in the first time and it does not matter how many white balls are selected in the remaining  $t-1$  times. The equation is as follows.

$$\begin{aligned}
P^t(k) &= G(0) \cdot P^{t-1}(k) + G(1) \cdot P^{t-1}(k-1) + \dots + G(k-1) \cdot P^{t-1}(1) + R(k) \\
&= \sum_{m=0}^{k-1} G(m) P^{t-1}(k-m) + R(k) \\
&= G(k) * P^{t-1}(k) + R(k),
\end{aligned} \tag{22}$$

$$\text{where } G(k) * P^{t-1}(k) = \sum_{m=0}^{k-1} G(m) P^{t-1}(k-m).$$

For the stage one of PENS, neighbor selection in each round is independent, so the probability remains unchanged in all rounds, we have

$$P^t(k) \equiv R(k). \tag{23}$$

## A.2 Proof of Corollary 1

Function  $Q(t)$  is defined as  $Q(t) = P^t(k)$ ,  $t \in \{1, \dots, T\}$ . To prove Corollary 1, we need to prove  $Q(t) - Q(t-1) > 0$ ,  $t \in \{2, \dots, T\}$ . We use Mathematical Induction method to prove the corollary.

**Step 1:**  $Q(t) - Q(t-1) > 0$  is satisfied when  $t = 2$ , because

$$\begin{aligned}
Q(2) - Q(1) &= P^2(k) - P^1(k) \\
&= G(k) * P^1(k) + R(k) - R(k) \\
&= G(k) * P^1(k) > 0.
\end{aligned} \tag{24}$$

**Step 2:** Assume  $Q(t) - Q(t-1) > 0$  when  $t = t$ , we now prove  $Q(t+1) - Q(t) > 0$  when  $t = t+1$ .

$$\begin{aligned}
Q(t+1) - Q(t) &= P^{t+1}(k) - P^t(k) \\
&= G(k) * P^t(k) + R(k) - (G(k) * P^{t-1}(k) + R(k)) \\
&= G(k) * P^t(k) - G(k) * P^{t-1}(k) \\
&= \sum_{m=0}^{k-1} G(m) P^t(k-m) - \sum_{m=0}^{k-1} G(m) P^{t-1}(k-m) \\
&= \sum_{m=0}^{k-1} G(m) [P^t(k-m) - P^{t-1}(k-m)].
\end{aligned} \tag{25}$$

We have  $Q(t) - Q(t-1) > 0$ , further

$$Q(t) - Q(t-1) = P^t(k) - P^{t-1}(k) > 0. \tag{26}$$

Therefore,

$$P^t(k-m) - P^{t-1}(k-m) > 0, \quad k > m. \tag{27}$$

Together with Equation (25) and (27), we can infer

$$Q(t) - Q(t-1) > 0. \tag{28}$$

**Step 3:** Based on Step 1 and 2, we can draw the conclusion that

$$Q(t) - Q(t-1) > 0, \quad \forall t \in \{2, \dots, T\} \tag{29}$$